Published in final edited form as:
Vision Res. 2012 December 15; 75: 98–107. doi:10.1016/j.visres.2012.09.011.

Evidence of a role of inositol polyphosphate 5-phosphatase INPP5E in cilia formation in zebrafish

Na Luo[A], **Jingping Lu**[A], and **Yang Sun**[A,B,*]

[A]Glick Eye Institute, Department of Ophthalmology, Indiana University School of Medicine, 1160 W. Michigan Street, Indianapolis, IN 46202

[B]Department of Dermatology, Indiana University School of Medicine, 1160 W. Michigan Street, Indianapolis, IN 46202

Abstract

Inositol phosphatases are important regulators of cell signaling and membrane trafficking. Mutations in inositol polyphosphate 5-phosphatase, INPP5E, have been identified in Joubert syndrome, a rare congenital disorder characterized by midbrain malformation, retinitis pigmentosa, renal cysts, and polydactyly. Previous studies have implicated primary cilia abnormalities in Joubert Syndrome, yet the role of INPP5E in cilia formation is not well understood. In this study, we examined the function of INPP5E in cilia development in zebrafish. Using specific antisense morpholino oligonucleotides to knockdown *Inpp5e* expression, we observed phenotypes of microphthalmia, pronephros cysts, pericardial effusion, and left-right body axis asymmetry. The *Inpp5e* morphant zebrafish exhibited shortened and decreased cilia formation in the Kupffer's vesicle and pronephric ducts as compared to controls. Epinephrine-stimulated melanosome trafficking was delayed in the *Inpp5e* zebrafish morphants. Expression of human INPP5E expression rescued the phenotypic defects in the *Inpp5e* morphants. Taken together, we showed that INPP5E is critical for the cilia development in zebrafish.

Keywords

Inositol phosphatase; primary cilia; Kupffer's vesicle; INPP5E; zebrafish

1. Introduction

The primary cilium is an evolutionarily conserved subcellular structure that protrudes from nearly all post-mitotic eukaryotic cells (Rohatgi & Snell, 2010). By sensing changes in the extracellular environment, the primary cilium can coordinate signaling cascades that subsequently become amplified throughout the cell (Fisch & Dupuis-Williams, 2011). A highly specialized extension of the plasma membrane, the ciliary membrane is enriched with many signaling precursors, such as Patched1 (Ptc1) (Corbit, et al., 2005, Rohatgi, et al., 2007). Upon ligand binding of Sonic Hedgehog (Hg), Ptc1 is removed from the cilium and Smoothened is then accumulated within the ciliary membrane, allowing initiation of

*corresponding author: sunyo@iupui.edu, Phone: 317-278-1878, Fax: 317-274-7744.

Conflict of Interest: None

downstream signaling cascades. The ciliary membrane covers a microtubule-based axoneme, which is anchored by a basal body (Pearson, et al., 2007, Pearson & Winey, 2009). Within the ciliary membrane are phospholipids, including phosphoinositides that may serve as second messengers in signal transduction. Defects in cilia formation or maintenance have been found to underlie a wide range of human diseases, including retinitis pigmentosa, renal cysts, polydactyly, and developmental delays, which are collectively called ciliopathies (Jacoby, et al., 2009, Novarino, et al., 2011, Schurman & Scheinman, 2009).

Joubert syndrome, a rare form of autosomal recessive ciliopathy, is characterized by an underdevelopment of cerebellar vermis, with a distinctive “molar tooth sign” of cerebellar vermis hypoplasia on MRI (Bielas, et al., 2009). The most common features of Joubert syndrome include retinitis pigmentosa, hypotonia, severe psychomotor delay, and ataxia (Lee & Gleeson, 2011). Other physical deformities may include polydactyly, cleft palate, renal cysts, and liver disease. A rapidly expanding number of genes have been implicated in Joubert syndrome, including NPHP1, NPHP6/CEP290, NPHP8, ARL13B and INPP5E (Arts, et al., 2007, Bielas et al., 2009, Cantagrel, et al., 2008, Kim, et al., 2008, McEwen, et al., 2007, Travaglini, et al., 2009, Valente, et al., 2010).

INPP5E belongs to a family of inositol polyphosphate 5-phosphatases, which dephosphorylate the D5 position of the inositol ring (Asano, et al., 1999, Kisseleva, et al., 2000, Kong, et al., 2000). There are ten mammalian members of the 5-phosphatase family, which play critical yet distinct roles in a number of biological processes, such as the regulation of insulin signaling, vesicular trafficking, synaptic vesicle formation, and hematopoietic cell proliferation (Ooms, et al., 2009, Pirruccello & De Camilli, 2012). The members of inositol polyphosphate 5-phosphatase family share a common inositol phosphatase domain, but these individual 5-phosphatases have different protein-protein interaction domains that regulate their subcellular localization and function (Dyson, et al., 2012). For instance, in response to growth factor stimulation, INPP5E regulates the intracellular levels of $PI(4,5)P_2$ and $PI(3,4,5)P_3$ by controlling downstream AKT activation (Kisseleva, et al., 2002). Overexpression of INPP5E also results in the hydrolysis of $PI(3,5)P_2$ to PI(3)P at the plasma membrane, and translocation of GLUT4 glucose transporter into the plasma membrane (Kong, et al., 2006). Mutations in the INPP5E phosphatase domain have been identified in a series of patients with Joubert syndrome, thus highlighting the role of inositol phosphatases in cilia development (Bielas et al., 2009). In addition, a C-terminal deletion mutant of INPP5E has been reported in a family with MORM syndrome, a variant of the Bardet-Biedel group of syndromic ciliopathies (Jacoby et al., 2009). *In vitro* studies revealed that the INPP5E deletion mutant failed to localize to the cilia while retaining its inositol phosphatase activity, thus suggesting that spatial localization of INPP5E, as well as enzymatic activity, is critical to its function in the cilia (Jacoby et al., 2009).

Although INPP5E has been implicated in ciliogenesis, the functional role of inositol phosphatase in the cilia is not understood. The murine model of MORM syndrome yielded knockout animals that died shortly after birth (Jacoby et al., 2009). Thus, to seek a viable INPP5E model system, we examined the function of INPP5E in zebrafish cilia development by transient knockdown with morpholino anti-sense oligonucleotides specific for *Inpp5e*.

2. Materials and Methods

2.1 Reagents and DNA constructs

Anti-acetylated α-tubulin and anti-Myc monoclonal antibodies were purchased from Sigma (St. Louis, MO). Mouse antibody against INPP5E antibody was obtained from Abcam (Cambridge, MA). Secondary antibodies were AlexaFluor 488 and 546-conjugated donkey

anti-mouse IgG, Cy3-conjugated donkey anti-mouse IgG, and horseradish peroxidase-conjugated goat anti-rabbit and anti-mouse IgG (Jackson ImmunoResearch Laboratories, Inc. West Grove, PA). IRDye goat anti-mouse and anti-rabbit (680 and 800) were obtained from Li-cor Bioscience (Lincoln, NB). Myc-tagged INPP5E was previously described (Kisseleva et al., 2002). Site-directed mutagenesis for INPP5E R378C and R435Q mutants was performed using QuikChange II (Aglient, Santa Clara, CA).

2.2 Immunoblot analysis

Cell lysates were subjected to SDS-PAGE followed by immunoblot analysis with the indicated antibodies. Equal amounts of protein were resolved on 10–12% polyacrylamide gels, and protein bands were transferred to nitrocellulose membranes (BioRad, Hercules, CA), which were blocked with 5% non-fat dried milk in PBST; and incubated with the primary and then secondary antibodies as indicated. Odyssey imaging system (Li-Cor Bioscience, Lincoln, NE) was used to analyze the immunoblots.

2.3 Zebrafish immunohistochemistry and cilia measurements

Zebrafish (wildtype strain: AB *tevbigan)* (gift of Dr. Ryan Anderson, Indiana University, Indianapolis, IN) were raised and maintained at the Laboratory Animal Resource Center of Indiana University. All animal procedures were subject to the Institutional Animal Care and Use Committee of Indiana University approved protocols. The phenotypes of morphants were photographed with Leica DFC310 FX. Eye size was determined by the longest diameter of eye area. The diameter was measured using Leica Appication Suite V4.1 and NIH Image J v1.46.

Embryos were fixed overnight at 4°C in 4% PFA and 1% sucrose in PBS. Embryos were dechorionated and washed with PBST for 6–8 times 10 min each. Following one hour of blocking with 10% NGS and 0.5% 0BSA, immunostaining was performed with 1:200 anti-acetylated α-tubulin monoclonal antibody and later with 1:500 Alexa Fluor 546 goat anti-mouse conjugated IgG at 4°C overnight. KV cilia measurements were performed as described (Luo et al., 2012). Cresyl violet staining was performed as described (Luo et al., 2012).

2.4 Morpholino (MO) antisense oligonucleotides knockdown and mRNA rescue in zebrafish

Antisense MOs were designed and purchased from Gene Tools, Inc (Gene Tools, Philomath, OR). The *Inpp5e* ATG initiation codon sequence is GCTCACTCATCCTATTGGCGGGCTT. A mismatch morpholino MO: sequence ATGCGAAATCAAGGTTCGATCATCA served as a negative control. We also used a *p53* ATG morpholino: GCGCCATTGCTTTGCAAGAATTG to test for off-target effects. Morpholino stocks were dissolved at 1 mM in water and 2 or 4 nl of injection solution (0.25% phenol red) containing 125–500 μM morpholino was injected into fertilized eggs at the one- to two-cell stage using a pressure injector, Pressure System IIe (Toohey Company, Fairfield, NJ). Synthetic mRNA was prepared from linearized human INPP5E-pcDNA3.1 DNA with Ambion mMessage mMachine® high-yield Capped RNA transcription kit, and purified with phenol-chloroform; mRNA was co-injected for rescue experiments.

2.5 Retrograde melanosome transport assay

The melanosome transport assay was performed as described (Yen, et al., 2006). Briefly, zebrafish 5 dpf larvae were exposed to epinephrine (50 mg/ml, Sigma) in the final concentration of 2 mg/ml in a dark room, and melanosome retractions were observed under

the brightfield microscope Leica DFC310 FX. The end of melanosome transport was marked when all melanosomes in the head were perinuclear.

2.6 Statistical analysis

Statistical analysis was performed using SPSS software (SPSS, Chicago, IL) and the p value less than 0.05 was considered significant. An unpaired t-test was carried out to analyze if there was a significant difference between the cilia length or percentage of cilia formation as described above. ANOVA test was performed to analyze the difference observed in different groups of hTERT-RPE1 cells transfected with INPP5E constructs.

3. Results

3.1 *Inpp5e* knockdown results in cilia-dependent phenotypes

Inositol metabolism has been explored in a number of model organisms, including zebrafish (*Danio rerio*) (Sarmah, et al., 2007). We have examined zebrafish orthologs of known inositol polyphosphate 5-phosphatases and identified the orthologous zebrafish *Inpp5e*. Human INPP5E contains an N-terminal proline-rich domain (PRD), an inositol polyphosphate 5-phosphatase domain, and a lipid modification domain (ie, CAAX) in the C-terminus (Figure 1A). Similarly, the zebrafish *Inpp5e* also contains a PRD, an inositol polyphosphate 5-phosphatase domain, and a CAAX domain. Known mutations in patients with Joubert syndrome are found within the 5-phosphatase domain, which is conserved between the human and zebrafish. Comparative studies of the protein sequence show 65% identity and 82% similarity between the human and zebrafish INPP5E. In the 5-phosphatase domain, there is 71% identity and 86% similarity between these two species (Figure 1B). The conserved amino acid sequences in the 5-phosphatase domains, FWFGDFNFR and KQRTPSYTDRVLY, are nearly identical in both human and zebrafish *Inpp5e* genes. Interestingly, the disease-causing mutations in humans are found in basic residues of arginine and lysine (R378, R435, R512, R515, R563, and K580), which are conserved in both species. However, an important difference is in the PRD, which contains 23% proline in the N-terminus of the human gene but only 11% in the zebrafish gene. In addition, the C-terminal prenylation signal, CAAX, is conserved in both species; CSVS is found in human INPP5E and CSIS is found in zebrafish *Inpp5e*, suggesting a conserved role of lipid modification in both zebrafish and humans.

To determine the functional significance of *Inpp5e* in cilia development, we established a zebrafish model by using antisense morpholino oligonucleotides to knockdown *Inpp5e* expression. To assess the *in vivo* effects of *Inpp5e* knockdown, we injected an *Inpp5e* translation-blocking morpholino and a mismatched control MO. As shown in Figure 2A, injection of *Inpp5e* morpholino specifically decreased Inpp5e protein expression as compared to β-actin; we verified *Inpp5e* expression by immunoblot analysis and demonstrated the specificity of INPP5E antibody. At 48 hpf stage, *Inpp5e* morphants exhibited phenotypes of microphthalmia, pericardial edema, body axis asymmetry, kinked tail, and pronephric cyst formation (Fig. 2B and Fig. 3A). Morphant embryos injected with increasing concentrations of *Inpp5e* MO demonstrated dose-dependent phenotypes in response to *Inpp5e* knockdown (Fig. 2C). Approximately 60% of morphants exhibited microphthalmia, which was observed over three independent sets of experiments (Fig. 2E). Many morphants also developed hypopigmentation and hydrocephalus (Fig. 2B and Fig. 3A).

To verify the phenotypes are specific to *Inpp5e* knockdown, we injected *p53* MO into zebrafish embryos and showed that *p53* MO alone did not result in either decreased eye size, generalized edema, or body axis asymmetry in zebrafish, but these phenotypes appeared in the embryos when co-injected with *p53* MO and *Inpp5e* MO (Fig. 2B). After measuring the

longest diameter of the eyes, we found a statistically significant decrease in eye size (unpaired t-test, p = 1.2E-08) at 48 hpf between *p53* morphants (247 μm ± 3.5 μm) and *p53* plus *Inpp5e* morphants (152 μm ± 11 μm) (Fig. 2D).

We examined the ocular phenotypes in detail and found the *Inpp5e* morphants exhibited abnormal retinal development compared to control zebrafish (Fig. 2F). The zebrafish larvae injected with control MO developed normal retinal structures with a well-defined nerve-fiber layer, inner nuclear and photoreceptor layers, but the *Inpp5e* MO-treated morphants exhibited disorganized retina with a lack of separation between the retinal cell layers. To examine the expression pattern of Inpp5e in the zebrafish retina, we performed immunofluorescence studies using anti-INPP5E antibodies. We confirmed the immunoreactivity of inositol phosphatase in the outer segment of photoreceptors; however, in zebrafish treated with *Inpp5e* MO, resulted in a loss of immunoreactivity in the eyes when compared to the controls (Fig. 2G).

To show that the body asymmetry, microphthalmia, and kinked tail are dependent on the loss-of-function of *Inpp5e*, we co-injected human INPP5E (hINPP5E) mRNA with *Inpp5e* MO to potentially rescue the observed phenotypes. Indeed, the expression of wildtype human INPP5E was able to partially rescue the loss-of-function of *Inpp5e*. The phenotypes of edema, body asymmetry and kinked tail reduced dramatically (Fig. 3A–B). The eye size of morphants co-injected with hINPP5E mRNA recovered to 215 μm ± 13 μm, compared with the morphants injected with *Inpp5e* MO (144 μm ± 14 μm) and control MO (253 μm ± 7.8 μm) (Fig 3C), thus supporting our hypothesis that the phenotypes observed are caused by the loss of *Inpp5e*.

3.2 Cilia defects in Kupffer's vesicle of *Inpp5e* morphants

To evaluate whether INPP5E is necessary for cilia development, we examined the Kupffer's vesicle (KV) of young larvae. The KV is a monociliated, fluid-containing structure in the zebrafish, orthologous to the mouse embryonic node (Hirokawa, et al., 2006). The KV is a spherical vesicle originating from dorsal forerunner cells and is readily visible in the tail-bud region. During early embryogenesis, the primary cilia within the KV generate directional flow just prior to the expression of asymmetric genes in the lateral cells. Previous studies have demonstrated that the ciliated KV is required for early somitogenesis for left-right patterning in the heart, gut, and the brain (Essner, et al., 2005, Kawakami, et al., 2005, Oteiza, et al., 2008). The cilia within the KV regulate left-right body axis and organ development, thus, we examined the KV by immunohistochemistry with anti-acetylated α-tubulin to stain the cilia at the 6-somite stage (Fig. 4A). *Inpp5e* morphants showed an approximate 50% decrease in the number of cilia within the KV (59 ± 3 in control embryos vs 35 ± 7 in *Inpp5e* morphants, unpaired t-test, t = 14.1, p = 0.02) when compared to control MO-injected embryos (Fig. 4B). In addition, the average length of cilia within the KV was found to be shorter in the *Inpp5e* morphants (2.9 μm ± 0.6 μm) as compared to controls (4.9 μm ± 0.4 μm) (unpaired t-test, t=12.4, p =1.56E-08) (Fig. 4C). Cilia formation in the KV can be rescued to a greater number (51 ± 5) and longer cilia length (4.3 μm ± 0.5 μm) after co-injection with hINPP5E mRNA. Thus, our results support that zebrafish *Inpp5e* function is required for KV cilia development.

3.3 Pronephric duct cilia defects of *Inpp5e* morphants

The pronephric kidney is the first stage of kidney development in vertebrate embryos (Otto, et al., 2003). Arising from the intermediate mesoderm, the pronephros has a single nephron that is attached to the nephric duct, which forms the Wolffian duct and ureter of the adult human kidney (Paces-Fessy, et al., 2012). In zebrafish, the primitive pronephros contains motile cilia that may generate flow by unidirectional beating (Essner, et al., 2002). It has

been shown that obstruction of fluid flow may result from the loss of ciliary function, leading to cystic kidney disease (Kramer-Zucker, et al., 2005). As cystic kidney has been implicated in human Joubert syndrome, we examined the zebrafish cilia in the pronephric ducts by immunofluorescence with anti-acetylated α-tubulin at the 24 hpf stage (Fig. 5A). As compared to control MO injected embryos, there was an approximate 50% shortening in the length of cilia of *Inpp5e* morphants (22 μm ± 2.1 μm) vs control embryos (10 μm ± 1.4 μm) (unpaired t-test, t = 21.3, p = 8.57E-08), and cilia could be rescued (18 μm ± 1.8 μm) by co-injection with hINPP5E mRNA (Fig. 5B). This finding may explain the phenotypes of renal cysts and generalized edema in the *Inpp5e* morphants. Our data supports that zebrafish *Inpp5e* function is involved in the cilia development in pronephric kidney.

3.4 Melanosome transport defects in *Inpp5e* morphants

In addition to KV and pronephros cilia, melanosome transport has been shown to be dependent on ciliary motor proteins (Yen et al., 2006). Melanosome shuttling between the cell periphery and the perinuclear region is mediated by kinesin II and dynein. Anterograde transport of the melanosomes to the cell periphery is caused by kinesin II motors while retrograde transport to the perinuclear region is performed by dyneins. Many ciliary proteins, such as BBS family members, are involved in retrograde melanosome transport in the zebrafish (Yen et al., 2006). Since we noted a pigmentary defect in the *Inpp5e* morphants (Fig. 2B and Fig. 3A), we hypothesized that melanosome transport may also be affected in the *Inpp5e*-deficient zebrafish. Retrograde or anterograde trafficking of melanosomes is known to be stimulated by epinephrine or caffeine, respectively (Nascimento, et al., 2003); therefore, we measured the rates of epinephrine-induced melanosome retraction in zebrafish morphants. In 5 dpf zebrafish larvae treated with epinephrine, the melanosomes contracted rapidly and perinuclear accumulation of melanosomes were observed (Fig. 6A). The pigment accumulation of *Inpp5e* morphants takes three times longer to complete than the control MO injected (6.0 ± 0.4 minutes in control vs 1.9 ± 0.2 minute in *Inpp5e* zebrafish, unpaired t-test, t = 28.9, p = 1.17E-18) (Fig. 6B). Moreover, the delayed melanosome retraction was partially rescued by co-injecting human INPP5E mRNA (Fig. 6B).

3.5 INPP5E mutants affect eye development in zebrafish

Recently INPP5E was identified in the connecting cilium in the photoreceptors of mice (Jacoby et al., 2009). In their INPP5E transgenic mice, short cilia development caused the absence of the photoreceptor cell layer. Almost all identified INPP5E mutations in Joubert syndrome are localized in the 5-phosphatase domain (Bielas et al., 2009). To examine the effect of mutant INPP5E on cilia formation during eye development, we first examined the localization of INPP5E mutants in the cilia of hTERT-RPE1 cells. In the hTERT-RPE1 cells expressing control vector, WT INPP5E, or mutant INPP5E R378C, and R435Q, we assessed the cilia length and percent of ciliated cells at 48 hours post serum-starvation. The cells transfected with mutant INPP5E R378C and R435Q have shortened cilia length and decreased cilia formation, thus suggesting these mutants may act as dominant negatives in cilia regulation (data not shown). We generated the mRNA of R378C and R435Q INPP5E mutants, which were co-injected with *Inpp5e* MO zebrafish embryos at the 1-cell stage. In zebrafish embryos injected with R378C and R435Q mRNA resulted in the phenotypes of generalized edema and body asymmetry (Fig. 7A). As shown in Fig. 7A and Fig. 7B, the zebrafish morphants injected with mutant INPP5E R378C and R435Q have smaller eyes (132 μm ± 20 μm in INPP5E R378C and 152 μm ± 18 μm in INPP5E R435Q) as compared to the zebrafish injected with wild type INPP5E (215 μm ± 13 μm) (unpaired t-test, p=3.6E-08). Taken together, we have showed that the disease-causing mutations in INPP5E affected cilia associated eye development.

4. Discussion

Lipid composition of the ciliary membrane is highly regulated. Phosphoinositide dysregulation has been implicated in ciliopathies in several recent studies (Bielas et al., 2009, Jacoby et al., 2009). INPP5E is an inositol 5-phosphatase involved in a cilia phenotype that underlies two rare human syndromic ciliopathies, Joubert syndrome and MORM syndrome, both of which present with retinal degeneration, kidney cysts, and mental developmental delays (Bielas et al., 2009, Jacoby et al., 2009). Studies in mice and humans have demonstrated that INPP5E plays a critical role in cilia function. In this study, we utilized zebrafish to examine the role of *Inpp5e* in the development of the cilium. The *Inpp5e* morphants develop ciliopathy-like phenotypes of hydrocephalus, retinal dysplasia, and body asymmetry, which is consistent with the murine knockout models. Since $Inpp5e^{\Delta/\Delta}$ mouse died soon after birth (Jacoby et al., 2009), the availability of a zebrafish model can provide a novel animal model to examine the role of inositol phosphatases in cilia development.

As previously shown in other ciliopathy studies, the zebrafish is a robust embryological model system to examine cilia function in early organogenesis (Chakarova, et al., 2011, Ghosh, et al., 2010, Hurd, et al., 2010, Khanna, et al., 2005, Murga-Zamalloa et al., 2010) because it offers optical clarity, rapid development, ease of genetic manipulation and high resolution imaging for *in vivo* studies that would not be achieved in larger animal models. Cilia function is required for maintaining left-right asymmetry and are conserved in nearly all vertebrates (Capdevila, et al., 2000). During early organogenesis, the left-right axis is maintained by asymmetric expression of LR-specific genes, such as *pitx2, nodal, lefty1* and *lefty2* (Hamada, et al., 2002). KV cilia are responsible for generating a transient left-biased calcium influx. The calcium flux is required for left-right determination (Schneider, et al., 2008). We show here that *Inpp5e* morphants exhibited left-right asymmetry as well as abnormal cilia formation in the KV, which support that INPP5E is a ciliary protein. Since $PI(4,5)P_2$ is the precursor for IP_3, which was shown to play a role in left-right body axis determination in Xenopus (Hatayama, et al., 2011), it is likely that the soluble inositol molecules may be the effectors for the body axis regulation.

The finding of pronephric duct cilia defects in *Inpp5e* morphants support the clinical observation of renal cyst development in human Joubert patients. The cilia within the pronephros in *Inpp5e* morphants were shorter and less organized than the control zebrafish, suggesting the motility of the cilia maybe severely affected. Cilia beating has been shown to be important in flow regulation in the pronephric ducts (Kramer-Zucker et al., 2005); the loss of cilia organization may reduce fluid movement resulting in cystic kidney formation. It will be important to visualize the ciliary beating in both the KV and pronephric ducts to determine if *Inpp5e* loss-of-function directly affects fluid transport in these embryonic structures.

Previously, Bielas *et al.* has shown that the fibroblasts from patients with mutations in the INPP5E 5-phosphatase domain exhibited ciliary instability (Bielas et al., 2009). Our results with the two disease-causing INPP5E mutants (R378C and R435Q) support this observation. In both mutants, we found that the cilia localization was unaffected by the loss of the inositol phosphatase activity. However, we did observe increased swelling of ciliary membrane at the distal tip of the cilia (unpublished results), suggesting the 5-phosphatase activity may play a role in retrograde transport of ciliary proteins. In addition to the enzymatic activity of INPP5E, the conservation of the C-terminal CAAX domain in both human and zebrafish INPP5E suggests that the lipid modification may play a vital role in the function of INPP5E in cilia. It will be important to identify the enzyme involved in this post-

translational modification; and the zebrafish will be an excellent model organism to test the functional importance of the CAAX domain.

Recently, three independent groups have identified another inositol polyphosphate phosphatase, OCRL, to also be involved in cilia function (Coon, et al., 2012, Luo et al., 2012, Rbaibi, et al., 2012). Mutations in OCRL are found in Lowe syndrome and Dent syndrome (Attree, et al., 1992, Lewis, 1993–2001, Reilly, et al., 1990). Lowe syndrome, also known as Oculocerebrorenal syndrome of Lowe, is a rare congenital X-linked recessive disorder characterized by congenital cataracts, glaucoma, renal tubular dysfunction, and developmental delays (Attree et al., 1992). Similar to Lowe syndrome, Type II Dent syndrome presents with congenital renal tubular dysfunction but lacks the ocular and cerebral phenotypes (Hoopes, et al., 2005, Schurman & Scheinman, 2009). OCRL was found to be trafficked to the cilia by Rab8 and Ses1/Ses2 and that the inositol phosphatase activity may be important in this ciliary recruitment (Coon et al., 2012). Another evidence for inositol regulation of cilia comes from studies of the tubby-like proteins. The tubby mouse, which develops adult-onset obesity, has mutations in the *Tub* gene; the tubby-like proteins are known to interact with phosphoinositides. Recently, Mukhopadhyay *et al.* has found Tubby-like protein 3 (TULP3) strongly binds to $PI(4,5)P_2$, followed by $PI(3,4)P_2$, and $PI(3,4,5)P_3$. Mutants of TULP3 that do not bind to phosphoinositides failed to traffic GPCR into the cilium (Mukhopadhyay, et al., 2010). Therefore, it was proposed that PIP_2 might regulate the specificity of trafficking of ciliary proteins.

In addition to lipid phosphoinositides, soluble inositol phosphates have been implicated in ciliogenesis and cilia-mediated signaling in zebrafish. Phosphoinositides Kinase 1 (PK1) is a 2-kinase that phosphorylates $I(1,3,4,5,6)P_5$ to generate IP_6 (Sarmah et al., 2007). Knockout of IPK1 in zebrafish resulted in loss of cilia maintenance as well as cessation of ciliary beating in the KV (Sarmah et al., 2007). Although the ultrastructure of the cilia does not appear disrupted, the functional transport of melanosomes implicated the loss of ciliary function. Immunofluorescence studies showed the distribution of IPK1 to the basal body in the cilia, suggesting a role of phosphorylation of IP_5 to IP_6 may be required in cilia function (Sarmah & Wente, 2010b). In addition to the direct cilia function, Sarmah *et al.* showed that higher order inositol phosphates are important in regulating Hg signaling, which is known to occur through the primary cilium. By knocking down IP6K2 expression in zebrafish, which prevents the formation of diphosphoryl inositol phosphates (PP-IPs), Sarmah *et al.* showed IP6K2 is a positive regulator of Hg signaling by acting upstream of transcription factor Gli1 (Sarmah & Wente, 2010a).

Although zebrafish offers a robust model system to examine the function of inositol metabolism in cilia formation, there are limitations to this approach. One of the drawbacks is the duration of Hg signaling the effectiveness of morpholinos; the degradation of the oligonucleotides over the first 48–72 hour period limits long-term studies of eye development and potential delayed phenotypes. Also, similar to the mouse model, another drawback is that the pleiotropic effect of *inpp5e* knockdown may result in early lethality of the zebrafish morphants. In the future, this may be circumvented by transplant technology, removing only the eyes into wild type zebrafish, which can allow specific examinations of ocular phenotypic rather than a global effect.

5. Conclusion

In this study, we present a knockdown zebrafish model using antisense morpholinos against *Inpp5e* that resemble human Joubert syndrome. This phenotype can be rescued by concomitant injection of normal human INPP5E mRNA. Following the knockdown of *Inpp5e*, we demonstrated a progressive loss of cilia at Kupffer's vesicle, pronephric kidney,

and subsequent alterations to organ laterality, such as bent body axes and cardiac left-right asymmetry. The high degree of homology between human and zebrafish INPP5E, and the rescue of human INPP5E shows that the zebrafish is a good model organism to study inositol phosphatase function in the cilia. The data presented supports a role for INPP5E in ciliary formation to explain the phenotypes in Joubert syndrome, and the knockdown zebrafish provides an animal model to test potential treatments in the future.

Acknowledgments

We thank Drs. Philip Majerus, Jeffrey Travers, Timothy Corson, Akhilesh Kumar, and Michael Conwell for thoughtful comments during the preparation of the manuscript. This work was funded by NIH K08 EY022058, a Pediatric Research Grant from the Knights Templar Eye Foundation, and a Clinician-Scientist award from American Glaucoma Society (Y.S.).

Abbreviations

RPE	retinal pigmented epithelium
NHF	normal human fibroblasts
MORM syndrome	mental retardation, truncal obesity, retinal dystrophy, and micropenis
RBD	RAB binding domain
ONL	outer nuclear layer
INL	inner nuclear layer
GCL	Ganglion cell layer
IFT	intraflagellar transport
hTERT-RPE1	human telomerase transformed RPE cells
PFA	paraformaldehyde
BSA	bovine serum albumin
NGS	Normal goat serum
PBS	phosphate buffered saline
FCS	fetal calf serum
PRD	proline rich domain
dpf	days post-fertilization
hpf	hours post-fertilization
KV	Kupffer’s vesicle

References

Arts HH, Doherty D, van Beersum SE, Parisi MA, Letteboer SJ, Gorden NT, et al. Mutations in the gene encoding the basal body protein RPGRIP1L, a nephrocystin-4 interactor, cause Joubert syndrome. Nat Genet. 2007; 39(7):882–888. [PubMed: 17558407]

Asano T, Mochizuki Y, Matsumoto K, Takenawa T, Endo T. Pharbin, a novel inositol polyphosphate 5-phosphatase, induces dendritic appearances in fibroblasts. Biochemical and biophysical research communications. 1999; 261(1):188–195. [PubMed: 10405344]

Attree O, Olivos IM, Okabe I, Bailey LC, Nelson DL, Lewis RA, et al. The Lowe’s oculocerebrorenal syndrome gene encodes a protein highly homologous to inositol polyphosphate-5-phosphatase. Nature. 1992; 358(6383):239–242. [PubMed: 1321346]

Bielas SL, Silhavy JL, Brancati F, Kisseleva MV, Al-Gazali L, Sztriha L, et al. Mutations in INPP5E, encoding inositol polyphosphate-5-phosphatase E, link phosphatidyl inositol signaling to the ciliopathies. Nat Genet. 2009; 41(9):1032–1036. [PubMed: 19668216]

Cantagrel V, Silhavy JL, Bielas SL, Swistun D, Marsh SE, Bertrand JY, et al. Mutations in the cilia gene ARL13B lead to the classical form of Joubert syndrome. Am J Hum Genet. 2008; 83(2):170–179. [PubMed: 18674751]

Capdevila J, Vogan KJ, Tabin CJ, Izpisua Belmonte JC. Mechanisms of left-right determination in vertebrates. Cell. 2000; 101(1):9–21. [PubMed: 10778851]

Chakarova CF, Khanna H, Shah AZ, Patil SB, Sedmak T, Murga-Zamalloa CA, et al. TOPORS, implicated in retinal degeneration, is a cilia-centrosomal protein. Hum Mol Genet. 2011; 20(5):975–987. [PubMed: 21159800]

Coon BG, Hernandez V, Madhivanan K, Mukherjee D, Hanna CB, Barinaga-Rementeria Ramirez I, et al. The Lowe syndrome protein OCRL1 is involved in primary cilia assembly. Human molecular genetics. 2012; 21(8):1835–1847. [PubMed: 22228094]

Corbit KC, Aanstad P, Singla V, Norman AR, Stainier DY, Reiter JF. Vertebrate Smoothened functions at the primary cilium. Nature. 2005; 437(7061):1018–1021. [PubMed: 16136078]

Dyson JM, Fedele CG, Davies EM, Becanovic J, Mitchell CA. Phosphoinositide phosphatases: just as important as the kinases. Sub-cellular biochemistry. 2012; 58:215–279. [PubMed: 22403078]

Essner JJ, Amack JD, Nyholm MK, Harris EB, Yost HJ. Kupffer's vesicle is a ciliated organ of asymmetry in the zebrafish embryo that initiates left-right development of the brain, heart and gut. Development. 2005; 132(6):1247–1260. [PubMed: 15716348]

Essner JJ, Vogan KJ, Wagner MK, Tabin CJ, Yost HJ, Brueckner M. Conserved function for embryonic nodal cilia. Nature. 2002; 418(6893):37–38. [PubMed: 12097899]

Fisch C, Dupuis-Williams P. Ultrastructure of cilia and flagella - back to the future! Biology of the cell/under the auspices of the European Cell Biology Organization. 2011; 103(6):249–270. [PubMed: 21728999]

Ghosh AK, Murga-Zamalloa CA, Chan L, Hitchcock PF, Swaroop A, Khanna H. Human retinopathy-associated ciliary protein retinitis pigmentosa GTPase regulator mediates cilia-dependent vertebrate development. Hum Mol Genet. 2010; 19(1):90–98. [PubMed: 19815619]

Hamada H, Meno C, Watanabe D, Saijoh Y. Establishment of vertebrate left-right asymmetry. Nature reviews Genetics. 2002; 3(2):103–113.

Hatayama M, Mikoshiba K, Aruga J. IP3 signaling is required for cilia formation and left-right body axis determination in Xenopus embryos. Biochemical and biophysical research communications. 2011; 410(3):520–524. [PubMed: 21683063]

Hirokawa N, Tanaka Y, Okada Y, Takeda S. Nodal flow and the generation of left-right asymmetry. Cell. 2006; 125(1):33–45. [PubMed: 16615888]

Hoopes RR Jr, Shrimpton AE, Knohl SJ, Hueber P, Hoppe B, Matyus J, et al. Dent Disease with mutations in OCRL1. Am J Hum Genet. 2005; 76(2):260–267. [PubMed: 15627218]

Hurd T, Zhou W, Jenkins P, Liu CJ, Swaroop A, Khanna H, et al. The retinitis pigmentosa protein RP2 interacts with polycystin 2 and regulates cilia-mediated vertebrate development. Hum Mol Genet. 2010; 19(22):4330–4344. [PubMed: 20729296]

Jacoby M, Cox JJ, Gayral S, Hampshire DJ, Ayub M, Blockmans M, et al. INPP5E mutations cause primary cilium signaling defects, ciliary instability and ciliopathies in human and mouse. Nat Genet. 2009; 41(9):1027–1031. [PubMed: 19668215]

Kawakami Y, Raya A, Raya RM, Rodriguez-Esteban C, Izpisua Belmonte JC. Retinoic acid signalling links left-right asymmetric patterning and bilaterally symmetric somitogenesis in the zebrafish embryo. Nature. 2005; 435(7039):165–171. [PubMed: 15889082]

Khanna H, Hurd TW, Lillo C, Shu X, Parapuram SK, He S, et al. RPGR-ORF15, which is mutated in retinitis pigmentosa, associates with SMC1, SMC3, and microtubule transport proteins. J Biol Chem. 2005; 280(39):33580–33587. [PubMed: 16043481]

Kim J, Krishnaswami SR, Gleeson JG. CEP290 interacts with the centriolar satellite component PCM-1 and is required for Rab8 localization to the primary cilium. Hum Mol Genet. 2008; 17(23):3796–3805. [PubMed: 18772192]

Kisseleva MV, Cao L, Majerus PW. Phosphoinositide-specific inositol polyphosphate 5-phosphatase IV inhibits Akt/protein kinase B phosphorylation and leads to apoptotic cell death. The Journal of biological chemistry. 2002; 277(8):6266–6272. [PubMed: 11706019]

Kisseleva MV, Wilson MP, Majerus PW. The isolation and characterization of a cDNA encoding phospholipid-specific inositol polyphosphate 5-phosphatase. J Biol Chem. 2000; 275(26):20110–20116. [PubMed: 10764818]

Kong AM, Horan KA, Sriratana A, Bailey CG, Collyer LJ, Nandurkar HH, et al. Phosphatidylinositol 3-phosphate [PtdIns3P] is generated at the plasma membrane by an inositol polyphosphate 5-phosphatase: endogenous PtdIns3P can promote GLUT4 translocation to the plasma membrane. Molecular and cellular biology. 2006; 26(16):6065–6081. [PubMed: 16880518]

Kong AM, Speed CJ, O'Malley CJ, Layton MJ, Meehan T, Loveland KL, et al. Cloning and characterization of a 72-kDa inositol-polyphosphate 5-phosphatase localized to the Golgi network. The Journal of biological chemistry. 2000; 275(31):24052–24064. [PubMed: 10806194]

Kramer-Zucker AG, Olale F, Haycraft CJ, Yoder BK, Schier AF, Drummond IA. Cilia-driven fluid flow in the zebrafish pronephros, brain and Kupffer's vesicle is required for normal organogenesis. Development. 2005; 132(8):1907–1921. [PubMed: 15790966]

Lee JE, Gleeson JG. Cilia in the nervous system: linking cilia function and neurodevelopmental disorders. Curr Opin Neurol. 2011; 24(2):98–105. [PubMed: 21386674]

Lewis RA, Nussbaum RL, Brewer ED. Lowe Syndrome. GeneReviews. 1993–2001 Jul 24.

Luo N, West CC, Murga-Zamalloa CA, Sun L, Anderson RM, Wells CD, et al. OCRL localizes to the primary cilium: a new role for cilia in Lowe syndrome. Human molecular genetics. 2012

McEwen DP, Koenekoop RK, Khanna H, Jenkins PM, Lopez I, Swaroop A, et al. Hypomorphic CEP290/NPHP6 mutations result in anosmia caused by the selective loss of G proteins in cilia of olfactory sensory neurons. Proc Natl Acad Sci U S A. 2007; 104(40):15917–15922. [PubMed: 17898177]

Mukhopadhyay S, Wen X, Chih B, Nelson CD, Lane WS, Scales SJ, et al. TULP3 bridges the IFT-A complex and membrane phosphoinositides to promote trafficking of G protein-coupled receptors into primary cilia. Genes & development. 2010; 24(19):2180–2193. [PubMed: 20889716]

Murga-Zamalloa CA, Atkins SJ, Peranen J, Swaroop A, Khanna H. Interaction of retinitis pigmentosa GTPase regulator (RPGR) with RAB8A GTPase: implications for cilia dysfunction and photoreceptor degeneration. Hum Mol Genet. 2010; 19(18):3591–3598. [PubMed: 20631154]

Nachury MV, Loktev AV, Zhang Q, Westlake CJ, Peranen J, Merdes A, et al. A core complex of BBS proteins cooperates with the GTPase Rab8 to promote ciliary membrane biogenesis. Cell. 2007; 129(6):1201–1213. [PubMed: 17574030]

Nascimento AA, Roland JT, Gelfand VI. Pigment cells: a model for the study of organelle transport. Annual review of cell and developmental biology. 2003; 19:469–491.

Novarino G, Akizu N, Gleeson JG. Modeling human disease in humans: the ciliopathies. Cell. 2011; 147(1):70–79. [PubMed: 21962508]

Ooms LM, Horan KA, Rahman P, Seaton G, Gurung R, Kethesparan DS, et al. The role of the inositol polyphosphate 5-phosphatases in cellular function and human disease. Biochem J. 2009; 419(1): 29–49. [PubMed: 19272022]

Oteiza P, Koppen M, Concha ML, Heisenberg CP. Origin and shaping of the laterality organ in zebrafish. Development. 2008; 135(16):2807–2813. [PubMed: 18635607]

Otto EA, Schermer B, Obara T, O'Toole JF, Hiller KS, Mueller AM, et al. Mutations in INVS encoding inversin cause nephronophthisis type 2, linking renal cystic disease to the function of primary cilia and left-right axis determination. Nature genetics. 2003; 34(4):413–420. [PubMed: 12872123]

Paces-Fessy M, Fabre M, Lesaulnier C, Cereghini S. Hnf1b and Pax2 cooperate to control different pathways in kidney and ureter morphogenesis. Human molecular genetics. 2012

Pearson CG, Culver BP, Winey M. Centrioles want to move out and make cilia. Dev Cell. 2007; 13(3): 319–321. [PubMed: 17765674]

Pearson CG, Winey M. Basal body assembly in ciliates: the power of numbers. Traffic. 2009; 10(5): 461–471. [PubMed: 19192246]

Pirruccello M, De Camilli P. Inositol 5-phosphatases: insights from the Lowe syndrome protein OCRL. Trends in biochemical sciences. 2012; 37(4):134–143. [PubMed: 22381590]

Rbaibi Y, Cui S, Mo D, Carattino M, Rohatgi R, Satlin LM, et al. OCRL1 modulates cilia length in renal epithelial cells. Traffic. 2012; 9999(999A)

Reilly DS, Lewis RA, Nussbaum RL. Genetic and physical mapping of Xq24–q26 markers flanking the Lowe oculocerebrorenal syndrome. Genomics. 1990; 8(1):62–70. [PubMed: 2081601]

Rohatgi R, Milenkovic L, Scott MP. Patched1 regulates hedgehog signaling at the primary cilium. Science. 2007; 317(5836):372–376. [PubMed: 17641202]

Rohatgi R, Snell WJ. The ciliary membrane. Current opinion in cell biology. 2010; 22(4):541–546. [PubMed: 20399632]

Sarmah B, Wente SR. Inositol hexakisphosphate kinase-2 acts as an effector of the vertebrate Hedgehog pathway. Proceedings of the National Academy of Sciences of the United States of America. 2010a; 107(46):19921–19926. [PubMed: 20980661]

Sarmah B, Wente SR. Zebrafish inositol polyphosphate kinases: new effectors of cilia and developmental signaling. Adv Enzyme Regul. 2010b; 50(1):309–323. [PubMed: 19914277]

Sarmah B, Winfrey VP, Olson GE, Appel B, Wente SR. A role for the inositol kinase Ipk1 in ciliary beating and length maintenance. Proc Natl Acad Sci U S A. 2007; 104(50):19843–19848. [PubMed: 18056639]

Schneider I, Houston DW, Rebagliati MR, Slusarski DC. Calcium fluxes in dorsal forerunner cells antagonize beta-catenin and alter left-right patterning. Development. 2008; 135(1):75–84. [PubMed: 18045845]

Schurman SJ, Scheinman SJ. Inherited cerebrorenal syndromes. Nat Rev Nephrol. 2009; 5(9):529–538. [PubMed: 19701229]

Travaglini L, Brancati F, Attie-Bitach T, Audollent S, Bertini E, Kaplan J, et al. Expanding CEP290 mutational spectrum in ciliopathies. Am J Med Genet A. 2009; 149A(10):2173–2180. [PubMed: 19764032]

Valente EM, Logan CV, Mougou-Zerelli S, Lee JH, Silhavy JL, Brancati F, et al. Mutations in TMEM216 perturb ciliogenesis and cause Joubert, Meckel and related syndromes. Nat Genet. 2010; 42(7):619–625. [PubMed: 20512146]

Yen HJ, Tayeh MK, Mullins RF, Stone EM, Sheffield VC, Slusarski DC. Bardet-Biedl syndrome genes are important in retrograde intracellular trafficking and Kupffer's vesicle cilia function. Hum Mol Genet. 2006; 15(5):667–677. [PubMed: 16399798]

Highlights

- We present a knockdown zebrafish model for inositol 5-phosphatase INPP5E
- Morphants defects of cilia in Kupffer's vesicle and pronephros ducts
- Wildtype human INPP5E can rescue the defect in zebrafish morphants

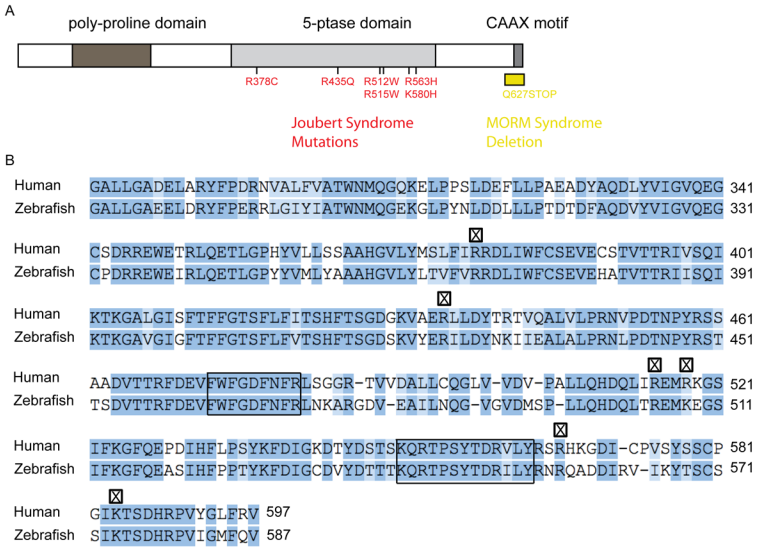

Figure 1. INPP5E in human and zebrafish

(A) Domain structure of human INPP5E. Known mutations in patients with Joubert syndrome (red) and MORM syndrome (yellow) are marked within the 5-phosphatase domain.

(B) Comparison of 5-phosphatase domain between human and zebrafish INPP5E. Conserved 5-phosphatase domain (boxed), and Joubert syndrome mutations (X) are indicated (summary based on (Jacoby et al., 2009) (Bielas et al., 2009)). Sequence alignment generated by Sequence Manipulation Suite (www.bioinformatics.org/sms2).

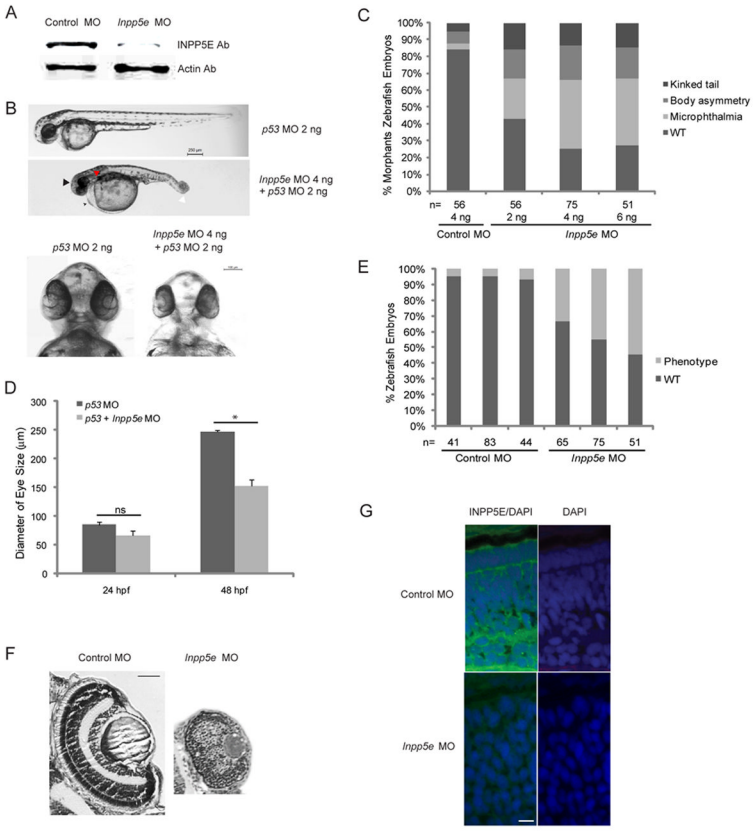

Figure 2. Phenotype of *Inpp5e* morphants

(A) Immunoblot analysis of 30 μg of total lysates of zebrafish embryo injected with control MO (4 ng) or *Inpp5e* MO (4 ng) at 48 hpf with anti-INPP5E and anti-β-actin antibodies.

(B) Zebrafish embryos were injected with *p53* MO (2 ng) or *p53* MO (2 ng) and *Inpp5e* MO (4 ng). Representative phenotypes of microphthalmia (black arrowhead), pericardial edema (small arrow), body axis asymmetry, kinked tail (white arrow), pronephric cyst formation (red arrow), and hypopigmentation were observed at 48 hpf (Top panel, scale bar 250 μm). The ventral sides of morphants are shown (Bottom, scale bar 100 μm).

(C) Dose-dependent effect of morpholinos in zebrafish. Control and *Inpp5e* MO at indicated doses were injected into zebrafish embryos, and phenotypes of microphthalmia, kinked tail, and body asymmetry were quantified at 48 hpf (ANOVA, F = 92, p = 3.6E-10), kinked tail (ANOVA, F = 3.6, p = 0.08), and body asymmetry (ANOVA, F = 5.2, p=0.04). (n = the number of injected embryos).

(D) Quantification of eye size of morphants at 24 hpf and 48 hpf. The eye size was determined by the longest diameters of eye balls in dorsal view. (n = 20 embryos, three independent experiments, unpaired t-test, * p = 1.2E-08, ns means not statistically significant).

(E) *Inpp5e* MO1 (4 ng) and control MO (4 ng) were injected into 1-cell zebrafish embryos. At 48 hpf, all the phenotypes were assessed and the total numbers of defective morphants in four independent experiments were quantified (n, the number of injected embryos, unpaired t-test, p=0.02).

(F) Cresyl violet staining of ocular sections of zebrafish larvae (5 dpf) injected with control MO (4 ng) or *Inpp5e* MO (4 ng). Scale bar 30 μm.

(G) Immunostaining of 3 dpf zebrafish larvae injected with control MO (4 ng) or *Inpp5e* MO (4 ng), followed by antibody staining against INPP5E (green) (DAPI, blue). Scale bar 10 μm.

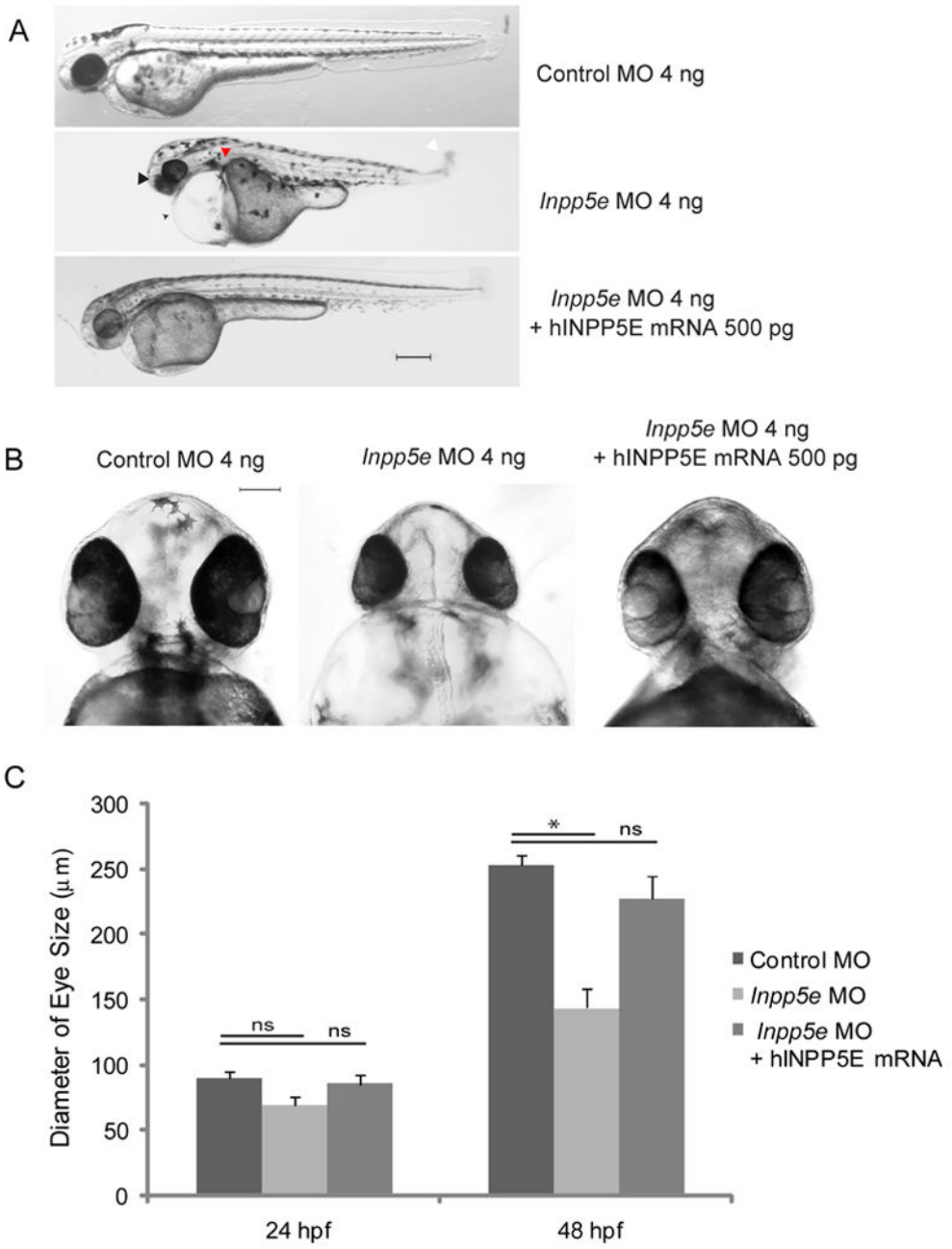

Figure 3. Human INPP5E rescue phenotypes of *Inpp5e* morphants

(A) Zebrafish embryos were injected with control MO (4 ng), *Inpp5e* MO (4 ng) or *Inpp5e* MO (4 ng) and human INPP5E mRNA (hINPP5E mRNA, 500 pg). Representative phenotypes of microphthalmia (arrowhead), pericardial edema (arrow), body axis asymmetry, kinked tail (white arrow), pronephric cyst formation (red arrow), and hypopigmentation were observed at 48 hpf (scale bar 250 μm).

(B) The ventral sides of embryos were injected with control MO (4 ng), *Inpp5e* MO (4 ng) or *Inpp5e* MO (4 ng) and human INPP5E mRNA (hINPP5E mRNA, 500 pg), scale bar 100 μm.

(C) Quantification of eye size of zebrafish morphants at 24 hpf and 48 hpf. (N=20 embryos, three independent experiments, unpaired t-test, * p = 1.61E-12).

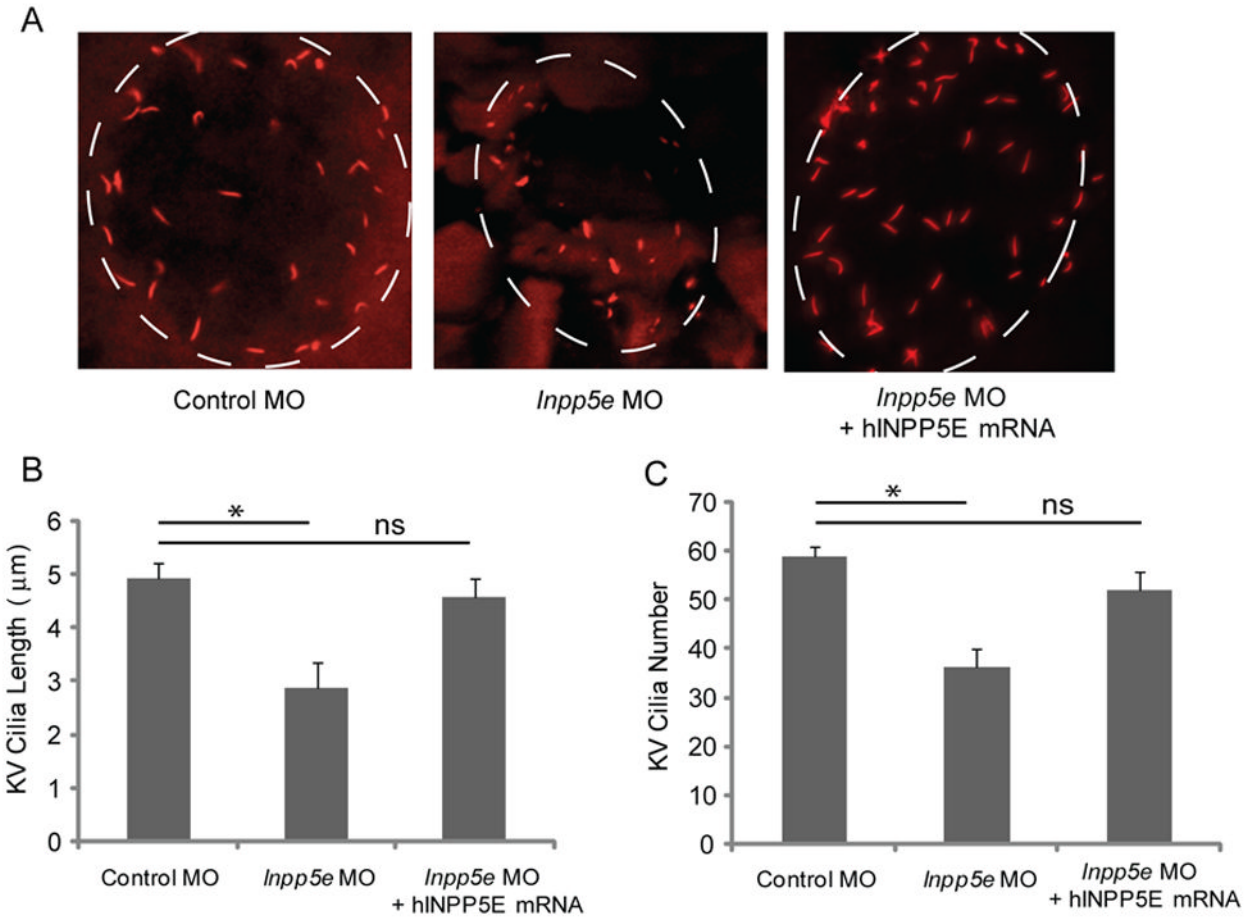

Figure 4. Kupffer's vesicle cilia defect in *Inpp5e* morphants

(A) Human INPP5E mRNA could rescue the loss of *Inpp5e*. KV cilia of zebrafish embryos injected with control MO (4 ng), *Inpp5e* MO (4 ng) or *Inpp5e* MO (4 ng) and hINPP5E mRNA (500 ng) at 6-somite stage were immunostained with acetylated α-tubulin (red), representative images are shown (dash line indicates border of KV).

(B–C) Quantification of number (B) and length (C) of KV cilia in zebrafish embryos injected with control MO (4 ng), *Inpp5e* MO (4 ng) or *Inpp5e* MO (4 ng) and hINPP5E mRNA (500 ng). (N=20 embryos, three independent experiments, unpaired t-test, * p = 0.02 in B and * p = 1.56E-08 in C).

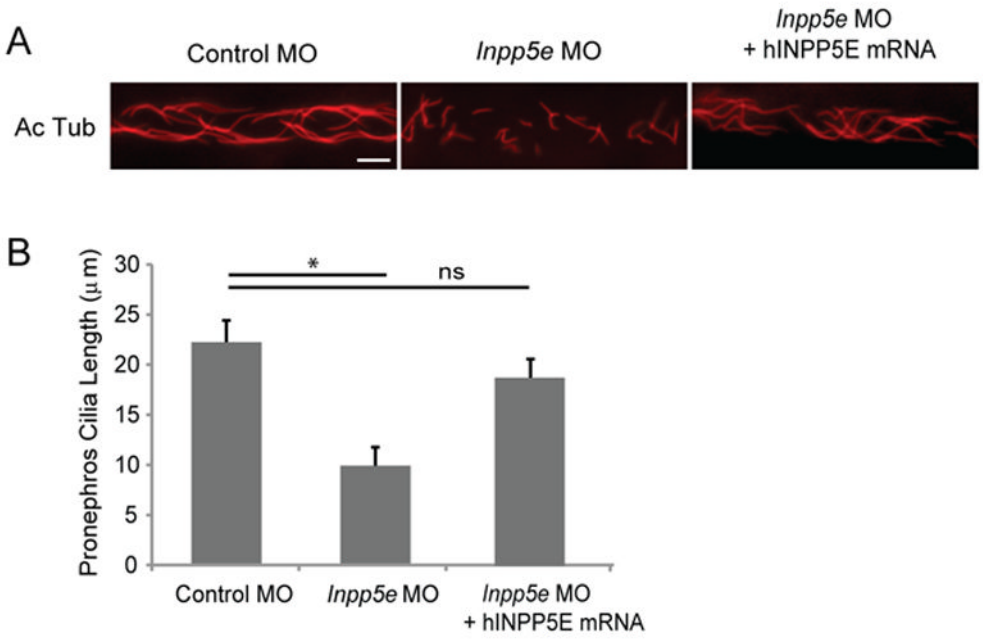

Figure 5. Pronephric cilia defect in *Inpp5e* morphants

(A) INPP5E mRNA rescue of *Inpp5e* pronephric cilia formation. Representative image of pronephric cilia of zebrafish embryos at 24 hpf stage, injected with control MO (4 ng), *Inpp5e* MO (4 ng) or *Inpp5e* MO (4 ng) and hINPP5E mRNA (500 ng), immunostaining with acetylated α-tubulin (red). Scale bar 10 μm.

(B) Pronephric cilia length of control and *Inpp5e* MO. Pronephric cilia of zebrafish embryos injected with control MO (4 ng), *Inpp5e* MO (4 ng) or *Inpp5e* MO (4 ng) and hINPP5E mRNA (500 ng) at 24 hpf stage were analyzed by immunostaining with acetylated α-tubulin and cilia length was measured. (N=20 embryos, three independent experiments, unpaired t-test, * p = 8.57E-08).

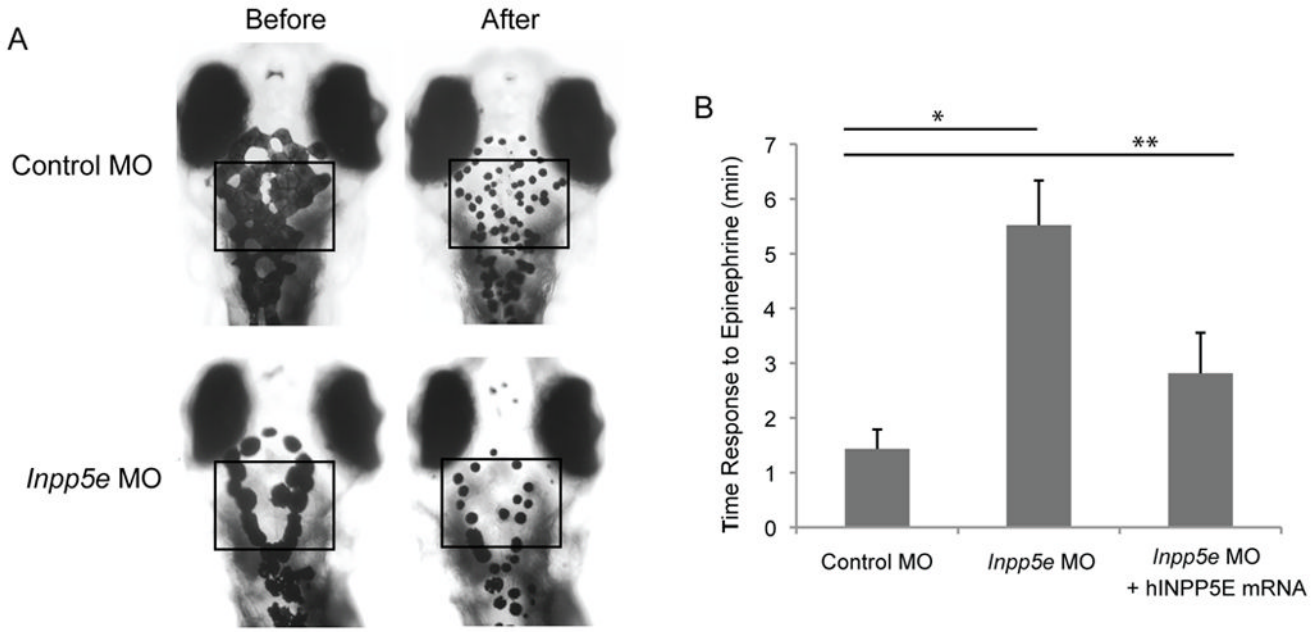

Figure 6. Impaired melanosome transport in *Inpp5e* morphants

(A) *Inpp5e* morphants showed slowed retrograde melanosome transport. Five day-old larvas injected with morpholinos were treated with epinephrine, and the time required for all melanosomes in the head and trunk to retract was determined. Representative photos are shown.

(B) Quantification of the response time for epinephrine treatments in the control MO (2 ng), *Inpp5e* MO (2 ng), and *Inpp5e* MO (2 ng) and hINPP5E mRNA (400 pg) embryos. (N=20 embryos, three independent experiments, unpaired t-test, * p = 1.17E-18, ** p = 1.5E-12).

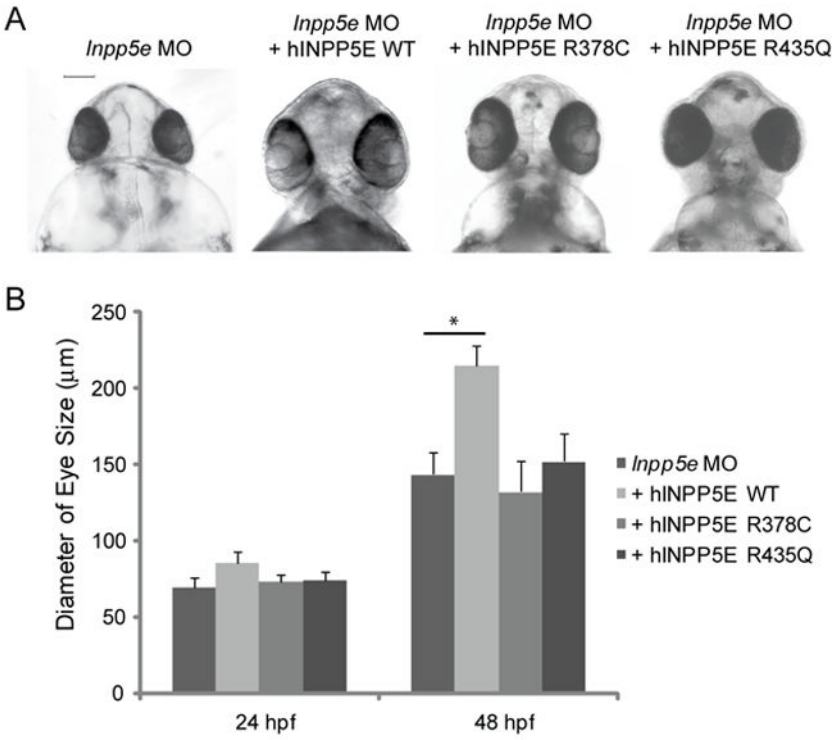

Figure 7. INPP5E mutants in zebrafish eye development

(A) Zebrafish embryos were injected with *Inpp5e* MO (4 ng), *Inpp5e* MO (4 ng) and hINPP5E WT mRNA (500 pg), *Inpp5e* MO (4 ng) and hINPP5E R378C mRNA (500 pg), or *Inpp5e* MO (4 ng) and hINPP5E R435Q mRNA (500 pg). The ventral sides of morphants are shown, scale bar 100 μm.

(B) Quantification of eye size of morphants at 24 hpf and 48 hpf. (N=20 embryos, three independent experiments, unpaired t-test, * p = 3.6E-08).